Mixed Quantum−Classical Scattering Dynamics of CF_3Br[†]

Nikola Marković*,[‡] and Andreas Bäck[§]

Physical Chemistry, Department of Chemistry and Bioscience, Chalmers University of Technology, SE-412 96 Göteborg, Sweden, and Department of Chemistry, Physical Chemistry, Göteborg University, SE-412 96 Göteborg, Sweden

Received: February 26, 2004; In Final Form: May 10, 2004

The vibrational excitation of CF_3Br scattering from graphite has been studied using mixed quantum−classical methods. A previously investigated 2D model for the intramolecular degrees of freedom [Bäck, A.; Marković, N. *Chem. Phys.* **2002**, *285*, 233] has been extended to 3D including all vibrations of a_1 symmetry, improving the dynamical description of the umbrella mode. We investigate the details of the excitation process for a few selected initial conditions as well as the general effect of surface temperature for ensembles of randomly sampled trajectories. Quantum results are obtained from 3D wave packet propagations and calculations based on the time-dependent Gauss−Hermite discrete variable representation method. When the quantum data are compared with classical results it is confirmed that quantization of the internal degrees of freedom does indeed have a very small effect for the present system. Considering vibrational excitation from the ground state, almost perfect agreement between quantum and classical calculations is found, provided that the classical trajectories are initialized without vibrational energy.

1. Introduction

Classical molecular dynamics (MD) simulation is a very powerful tool within the field of physical chemistry and chemical physics. The technique can provide information about hard-to-measure dynamical details as well as predictions of averaged experimental quantities. Both these aspects are illustrated in our previous work on the scattering of xenon atoms[1] and large water clusters[2] from graphite. These calculations involve many atoms and long propagation times and would be very hard to carry out using more sophisticated dynamical methods. Fortunately, we believe that a classical mechanical description is adequate for the studied processes, which is also supported by the good agreement with experimental results. We have also investigated vibrational excitation of polyatomic molecules scattering from hot graphite surfaces.[3−5] Due to the large energy gaps between vibrational energy levels one may expect quantum effects to be important for such processes, in particular for systems with high-frequency vibrations.

In ref 4 we obtained good agreement between experimental and simulated results for vibrational excitation of CF_3Br scattering from graphite for collision energies between 0.6 and 3.5 eV and surface temperatures between 500 and 1200 K. Due to the rather approximate potentials used and average character of the experimental measurements the agreement only indicates that a classical treatment is valid. The fact that the system is heavy and the frequencies rather low supports the use of classical mechanics. The observed sensitivity of the vibrational excitation to the methods of initialization and analysis, on the other hand, indicate that quantum effects still may play a role. In a recent paper we studied the system using a reduced dimensionality treatment including the C−Br stretch and the CF_3 umbrella motion.[6] Within this 2D approximation we could afford to carry out wave packet calculations to be compared with the corresponding classical treatment. One of the main conclusions was that the classical excitation of an initially nonvibrating molecule was almost identical to the quantum dynamical excitation from the vibrational ground state. Comparison of the 2D results with full-dimensional trajectory results (and also with experimental data) was, however, somewhat hampered by the artificial dynamical constraints invoked.

In the present paper those constraints are relaxed. In addition to the C−Br stretch (ν_3) and the umbrella motion (ν_2) we also include the C−F stretch (ν_1). Thus all three modes of a_1 symmetry are considered. The three modes have quite different vibrational frequencies, 352(ν_3), 762(ν_2), and 1085(ν_1) cm^{-1}, respectively, and quantum effects are therefore expected to influence them differently. The effect of the previously used constraints on the classical dynamics is investigated first. The collisional dynamics for a few selected initial geometries are studied in detail on a cold surface using both classical and wave packet methods. Some of these orientations only excite the a_1 vibrations due to symmetry reasons and therefore correspond to a full-dimensional treatment of the intramolecular dynamics. The quantum dynamical problem is also reformulated using the time-dependent Gauss−Hermite discrete variable representation method (TDGH-DVR), also known as quantum dressed classical mechanics,[7−16] replacing the reduced dimensionality treatment with a mixed quantum/classical description of the intramolecular dynamics. The wave packet and classical models are finally used to compute the surface temperature dependence of the vibrational excitation.

The dynamical model, the potentials used, and the theoretical methods are described in section 2. The results are presented in section 3, and the main conclusions are finally summarized in section 4.

2. Theory

The potential functions used in the present work are identical to those described in ref 4. The interaction between the 150

[†] Part of the "Gert D. Billing Memorial Issue".

* Corresponding author. E-mail: nikola@chembio.chalmers.se.
[‡] Chalmers University of Technology.
[§] Göteborg University.

10.1021/jp049138k CCC: $27.50 © 2004 American Chemical Society
Published on Web 06/16/2004

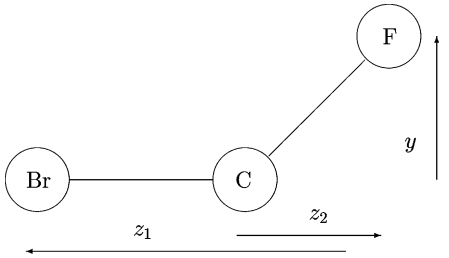

Figure 1. Definition of the coordinates used in the reduced dimensionality calculations.

carbon atoms in one of the five graphite sheets is given by Brenner's empirical function,[17] while the interlayer potential is modeled as a sum of Morse potentials. The bottom layer is held fixed, and the atoms in the next layer are subject to stochastic and friction forces in order to keep the graphite at a specified temperature. The gas−surface potential consists of a sum of Lennard-Jones terms yielding a binding energy of 0.27 eV. The intramolecular CF_3Br potential is described in terms of Morse stretch and attenuated harmonic bend and nonbonded interactions. The intramolecular potential reproduces the experimental normal mode frequencies: $\tilde{\nu}_1 = 1084.8$, $\tilde{\nu}_2 = 762.0$, $\tilde{\nu}_3 = 352.1$, $\tilde{\nu}_4 = 1208.8$, $\tilde{\nu}_5 = 547.4$, $\tilde{\nu}_6 = 302.7$ cm^{-1}, where the first three modes are nondegenerate of a_1 symmetry and the last three are doubly degenerate.

2.1. Reduced Dimensionality Wave Packet Calculations. The present reduced dimensionality calculations are carried out in terms of the distance between Br and the center of mass of CF_3 (z_1), the distance between C and the plane of the F atoms (z_2), and the distance from the Br−*C* axis to the F atoms (y), see Figure 1. As in our previous work with the umbrella model,[6] C_{3v} symmetry is preserved, but now also the C−F distance is allowed to change.

The intramolecular Hamiltonian in these coordinates is given by[18]

$$\hat{H}_{\mathrm{vib}} = -\frac{\hbar^2}{2\mu_1}\frac{\partial^2}{\partial z_1^{\,2}} - \frac{\hbar^2}{2\mu_2}\frac{\partial^2}{\partial z_2^{\,2}} - \frac{\hbar^2}{2\mu_3}\frac{\partial^2}{\partial y^2} + V(z_1, z_2, y) \quad (1)$$

where

$$\mu_1 = \frac{m_{\mathrm{Br}}(m_{\mathrm{C}} + 3m_{\mathrm{F}})}{m_{\mathrm{Br}} + m_{\mathrm{C}} + 3m_{\mathrm{F}}} \quad (2)$$

$$\mu_2 = \frac{3m_{\mathrm{C}}m_{\mathrm{F}}}{m_{\mathrm{C}} + 3m_{\mathrm{F}}} \quad (3)$$

$$\mu_3 = 3m_{\mathrm{F}} \quad (4)$$

This Hamiltonian exactly reproduces the nondegenerate normal mode frequencies, in contrast to the 2D Hamiltonian used in our previous study[6] which overestimated the umbrella frequency, ν_2, by ca. 7%. The translation and rotation of the molecule as well as the motion of the surface atoms are treated classically. The total Hamiltonian thus takes the form

$$\hat{H} = \frac{1}{2M}(P_X^{\,2} + P_Y^{\,2} + P_Z^{\,2}) + \hat{H}_{\mathrm{vib}}(z_1, z_2, y) + H_{\mathrm{rot}}(\phi, \theta, \chi, p_\phi, p_\theta, p_\chi, z_1, z_2, y) + V_{\mathrm{gs}}(X, Y, Z, z_1, z_2, y, \phi, \theta, \chi, \{q_{\mathrm{s}}\}) + H_{\mathrm{surf}}(\{q_{\mathrm{s}}\}, \{p_{\mathrm{s}}\}) \quad (5)$$

where M is the mass of the molecule, X, Y, Z specifies its center of mass, and ϕ, θ, χ are Euler angles describing its orientation. The gas−surface potential is denoted by V_{gs}, and the classical Hamiltonian for the surface atoms by H_{surf}. The rotational Hamiltonian is expressed as

$$H_{\mathrm{rot}} = \frac{L_x^{\,2}}{2I_{xx}} + \frac{L_y^{\,2}}{2I_{yy}} + \frac{L_z^{\,2}}{2I_{zz}} \quad (6)$$

where $I_{\alpha\alpha}$ are the principal moments of inertia which depend on the quantum coordinates z_1, z_2 and y. The body-fixed angular momenta, L_α, can be expressed in terms of the Euler angles and conjugate momenta

$$\begin{aligned} L_x &= -p_\phi \csc\theta \cos\chi + p_\theta \sin\chi + p_\chi \cot\theta \cos\chi \\ L_y &= p_\phi \csc\theta \sin\chi + p_\theta \cos\chi - p_\chi \cot\theta \sin\chi \\ L_z &= p_\chi \end{aligned} \quad (7)$$

The quantum part of the problem is solved by propagating the solution to the time-dependent Schrödinger equation

$$i\hbar\frac{\partial\Psi(z_1, z_2, y, t)}{\partial t} = \hat{H}_{\mathrm{Q}}\Psi(z_1, z_2, y, t) \quad (8)$$

where all terms with explicit dependence on the quantum variables are included in $\hat{H}_{\mathrm{Q}}$

$$\hat{H}_{\mathrm{Q}} = \hat{H}_{\mathrm{vib}} + H_{\mathrm{rot}} + V_{\mathrm{gs}} \quad (9)$$

The simultaneous propagation of the classical equations of motion for translation, rotation, and the motion of the surface atoms is carried out using an effective (mean-field) Hamiltonian

$$H_{\mathrm{eff}} = \langle\Psi|\hat{H}|\Psi\rangle \quad (10)$$

The initial wave packet (corresponding to the vibrational ground state in the present study) is an eigenfunction to the Hamiltonian in eq 1 obtained by expanding the vibrational wave function in a product of Morse eigenfunctions and solving the corresponding eigenvalue problem. The solution to eq 8 is propagated in time using the split-operator method[19] with the kinetic energy operators evaluated using the fast Fourier transform technique.[20] A modest grid consisting of $28 \times 28 \times 24$ points for (z_1, z_2, y) was found to be adequate for this problem. The classical degrees of freedom were propagated using a time step of 0.3 fs, while 0.1 fs was used for the quantum propagation. The molecule was placed with its center of mass 9.5 Å from the surface with the initial velocity vector (usually corresponding to a translational energy of 2.0 eV) in the negative normal direction.

The results of primary interest are the total vibrational energy

$$E_{\mathrm{vib}} = \langle\Psi|\hat{H}_{\mathrm{vib}}|\Psi\rangle \quad (11)$$

and its partitioning between the three vibrational modes (ν_3, ν_2, ν_1)

$$E_{\mathrm{vib}}(\nu_3) = \sum_i E_{i,0,0}\sum_{j,k} P_{i,j,k} \quad (12)$$

$$E_{\mathrm{vib}}(\nu_2) = \sum_j E_{0,j,0}\sum_{i,k} P_{i,j,k} \quad (13)$$

$$E_{\mathrm{vib}}(\nu_1) = \sum_k E_{0,0,k}\sum_{i,j} P_{i,j,k} \quad (14)$$

assuming approximate separability which makes an assignment to different modes possible. The summations are over 100 projections onto vibrational eigenstates, $P_{i,j,k}$, and using the

corresponding eigenvalues, $E_{i,j,k}$, up to a maximum energy of 689 meV. Due to vib−rot coupling it is necessary to compute average vibrational energies before and after the scattering event, i.e., when the molecule is approaching (leaving) the surface but before (after) the gas−surface interaction is significant.

The quantum results obtained using the wave packet method have been compared to the corresponding results from classical trajectories using the same reduced dimensionality treatment. The mode-resolved energies are in the classical case obtained by projecting the vibrational velocity vector onto the normal mode eigenvectors. The kinetic energy in the normal modes are averaged over time, and the mode-resolved vibrational energy is finally approximated as twice the kinetic average, which is a good approximation for the small excitations typical for the present system.

2.2. TDGH-DVR Calculations. The quantum dressed classical mechanics calculations are built around the full-dimensional classical trajectory program used in ref 4. We will sometimes refer to the full-dimensional calculations as "9D" since all nine intramolecular vibrations are considered. The propagation is carried out in terms of the Cartesian coordinates for the atoms. At every time step the Euler angles describing the orientation of the molecule are calculated, the normal mode eigenvectors are rotated accordingly, and values for the normal mode coordinates, Q_k, and conjugate momenta, P_k, are obtained. This procedure allows us to compute classical mode-resolved vibrational energies, but in addition we can distribute grid points around the classical Q_k values and treat the normal coordinates quantum mechanically within the time-dependent Gauss−Hermite discrete variable representation method. The method has been described in detail by Billing (see, e.g., refs 8−10). Below follows a brief summary of the equations used in the calculations.

For each degree of freedom, k, treated quantum mechanically an odd number, n_k, of points, $Q_{k,i}$, are distributed around the classical value, $Q_k(t)$ (the midpoint)

$$Q_{k,i} = Q_k(t) + z_i\sqrt{\frac{\hbar}{2\ \mathrm{Im}\ A_k(t)}} \tag{15}$$

where z_i are the zeros of the n_kth Hermite polynomial, $H_{n_k}(\xi)$. The roots z_i are found using the algorithm suggested by Billing.[8] The quantity A_k is a parameter defining the width of the Gauss−Hermite basis functions, ψ_n, which have the general form

$$\psi_n(Q_k, t) = \pi^{1/4}\exp\left\{\frac{\mathrm{i}}{\hbar}[\gamma_k(t) + P_k(t)(Q_k - Q_k(t)) + \mathrm{Re}\ A_k(t)(Q_k - Q_k(t))^2]\right\}\phi_n(\xi, t) \tag{16}$$

where

$$\phi_n(\xi, t) = \frac{1}{\sqrt{n!2^n\pi^{1/2}}}H_n(\xi)\exp(-\xi^2/2) \tag{17}$$

The time dependence follows from the relation

$$\xi = \sqrt{2\ \mathrm{Im}\ A_k(t)/\hbar}(Q_{k,i} - Q_k(t)) \tag{18}$$

The Gauss−Hermite functions are orthonormal if we require that

$$\mathrm{Im}\ \gamma_k(t) = -\frac{\hbar}{4}\ln(2\ \mathrm{Im}\ A_k(t)/\pi\hbar) \tag{19}$$

Since the transition probabilities do not depend on the phase factor, Re γ_k, its value is irrelevant. In our implementation we will furthermore set Re $A(t) = 0$ and keep it zero which implies that also Im A_k is kept constant.[14,21]

The total number of grid points is given by

$$N_{\mathrm{tot}} = \prod_{k=1}^{N} n_k \tag{20}$$

where N is the number of quantum degrees of freedom. The amplitudes at the grid points at $t = 0$ are given by

$$d_{i_1,i_2,\ldots,i_N}(0) = \left(\frac{\hbar}{2}\right)^{N/4}\left(\prod_{k=1}^{N}\mathrm{Im}\ A_k\right)^{-1/4}\prod_{k=1}^{N}\frac{g_v^{\,k}(Q_{k,i})}{\sqrt{\mathcal{N}_i^k}} \tag{21}$$

where $g_v(Q)$ is a vibrational eigenfunction and $\mathcal{N}_i^k$ a normalization factor

$$\mathcal{N}_i^k = \sum_{n=0}^{n_k-1}\phi_n(z_i)^2 \tag{22}$$

The amplitudes are propagated in time using the matrix equation

$$\mathrm{i}\hbar\ \dot{\mathbf{d}}(t) = (\mathbf{W}(t) + \mathbf{T})\ \mathbf{d}(t) \tag{23}$$

The potential matrix $\mathbf{W}$ is diagonal in the grid representation and obtained by subtracting the first and second derivative terms, evaluated at the classical trajectory, from the potential at the specific grid point

$$W(\{Q_{k,i}\}) = V(\{Q_{k,i}\}) - \sum_{k=1}^{N}\left.\frac{\partial V}{\partial Q_k}\right|_{Q(t)}(Q_{k,i} - Q_k(t)) - \sum_{k=1}^{N}\left.\frac{\partial^2 V}{\partial Q_k^{\,2}}\right|_{Q(t)}(Q_{k,i} - Q_k(t))^2 \tag{24}$$

where the derivative terms are given by ($m_k = 1$ in our case)

$$\frac{\partial V}{\partial Q_k} = -\dot{P}_k(t) \tag{25}$$

$$\frac{\partial^2 V}{\partial Q_k^{\,2}} = 4(\mathrm{Im}\ A_k)^2/m_k \tag{26}$$

The first derivative in eq 25 is the classical force, and the equation is simply one of the classical equations of motion. Since we do not integrate Q_k and P_k explicitly (the calculation proceeds in Cartesian coordinates) we prefer to determine the derivative from the time dependence of P_k using numerical differentiation. The accuracy of the method has been checked by comparison with explicit evaluation of the gradient of the potential with respect to the normal coordinates using the chain rule. For simple cases the explicit method is as easy to use as numerical differentiation, but for more general cases (involving rotation) the latter method is much simpler. The second derivative in eq 26 is not equal to the corresponding classical quantity. The effective forces, V' and V'', are in principle arbitrary.[10] The particular choice of V'' (combined with the requirement that Re $A_k(0) = 0$) guarantees that the width parameter Im A_k is time-independent, i.e., the grid points follow the classical trajectory with constant separation between the points. The kinetic coupling matrix $\mathbf{T}$ is sparse. The elements, which couples grid

points (i,j) in mode p are given by

$$T_{i(p)j(p)} = \prod_{q\neq p}\delta_{k(q)l(q)}\frac{\hbar \operatorname{Im} A_p}{m_p}\frac{1}{\sqrt{\mathcal{N}_i^p \mathcal{N}_j^p}}\sum_{n=0}^{n_p-1}\phi_n(z_i)(2n+1)\phi_n(z_j) \tag{27}$$

where $k^{(q)}$, $l^{(q)}$ denotes two grid points in mode q. An algorithm for the evaluation of the action of **T** on the vector **d** is given in ref 16. We have tested our implementation of the algorithm in two dimensions, where explicit expressions are easy to write down.[10] The solution to eq 23 can formally be written as

$$\mathbf{d}(t+\Delta t) = \exp\left(-\frac{\mathrm{i}}{\hbar}(\mathbf{W}(t)+\mathbf{T})\Delta t\right)\mathbf{d}(t) \tag{28}$$

The fact that the matrix is diagonally dominant suggests the splitting[22]

$$\mathbf{d}(t+\Delta t) = \exp\left(-\frac{\mathrm{i}}{2\hbar}\mathbf{E}(t)\Delta t\right)\exp\left(-\frac{\mathrm{i}}{\hbar}\mathbf{C}\Delta t\right)\exp\left(-\frac{\mathrm{i}}{2\hbar}\mathbf{E}(t)\Delta t\right)\mathbf{d}(t) \tag{29}$$

where the diagonal matrix **E** contains **W** and the diagonal part of the kinetic coupling **T**, whereas the nondiagonal part of the kinetic coupling is stored in **C**. The Lanczos method[23] is then used to propagate the vector

$$\exp\left(-\frac{\mathrm{i}}{2\hbar}\mathbf{E}(t)\Delta t\right)\mathbf{d}(t) \tag{30}$$

using the matrix **C**.

The classical trajectory is initialized without vibrational energy which corresponds to $Q_k = 0$ and $P_k = 0$. Grids are set up for those modes (ν_3, ν_2, and ν_1 in the present study) treated quantum mechanically, and initial quantum amplitudes are calculated from eq 21 using harmonic oscillator eigenfunctions. The classical equations of motion and the solution to the quantum problem are propagated simultaneously. The vibrational energy in the modes treated quantum mechanically is obtained by projecting the wave function onto asymptotic eigenstates. The amplitude corresponding to a final state characterized by the quantum numbers $\{v_f\}$ is obtained as

$$a_{\{v_f\}} = \left(\frac{\hbar}{2}\right)^{N/4}\left(\prod_{k=1}^{N}\operatorname{Im} A_k\right)^{-1/4}\sum_{i_1,\ldots,i_N}\prod_{k=1}^{N}\frac{g_{v_f}^{k}(Q_{k,i})}{\sqrt{\mathcal{N}_i^k}}\exp\left(\frac{\mathrm{i}}{\hbar}\sum_{k=1}^{N}P_k(t)(Q_{k,i}-Q_k(t))\right)d_{i_1,i_2,\ldots,i_N} \tag{31}$$

The probability is given by $P_{\{v_f\}} = |a_{\{v_f\}}|^2$, the total vibrational energy is obtained as

$$E_{\mathrm{vib}} = \sum_{\{v_f\}}E_{\{v_f\}}P_{\{v_f\}} \tag{32}$$

and the mode-resolved energies, finally, are found using eqs 12−14.

We have tested our implementation of the TDGH-DVR subroutines on the problem of rotational excitation in the He + H_2 system considered previously by Billing.[9,22] The results are not sensitive to the time step or the number of Lanczos recursions. Values between 0.1 and 0.5 fs together with five recursions using the split-Lanczos method is sufficient. We did, however, notice that the maximum stable propagation time seemed to be correlated with the number of grid points. Following the transition probabilities as a function of time we observed that reasonable values were obtained immediately after the collision but that the probabilities started to behave erratically if the propagation continued for too long. Increasing the number of recursions or decreasing the time step did not improve the situation. Adding grid points, however, removed the oscillations in addition to improving the accuracy of the probabilities obtained. The same behavior was observed for the CF_3Br system but did not pose a problem once we were aware of it. In all calculations presented we used the width parameter $\operatorname{Im} A_k = 0.0591$ u^2/fs (remember that the normal coordinates are mass-weighted). A peculiarity of the CF_3Br system is that for some—but not all—collisions we observe small unphysical oscillations in the transition probabilities. The oscillations were found to coincide with high classical kinetic energy in the vibrations. We therefore monitor this energy term and limit the projection to times when the kinetic energy has a minimum.

3. Results and Discussion

3.1. Scattering from a Cold Surface. In this section classical and quantum results obtained using the reduced dimensionality formulation are compared for a few specific initial molecular orientations. Three of these are particularly interesting since only a_1 vibrations are excited due to symmetry constraints. The results obtained therefore correspond to a full-dimensional dynamical treatment. For these cases we have also carried out calculations using the TDGH-DVR method. A zero K graphite surface was used in order to minimize the effects of thermal fluctuations. The translational energy was 2.0 eV (corresponding to 1615 m/s) and the initial velocity vector was along the surface normal. The initial orientations are the same as in ref 6 (Θ is the angle between the C−Br vector and the surface normal):

(i) the Br and C atoms are centered above a six-membered ring with the F atoms pointing down toward carbon atoms ($\Theta = 0°$);

(ii) the F atoms are approximately above the carbon atoms with the C and Br atoms centered above a six-membered ring and the Br atom turned downward ($\Theta = 180°$);

(iii) the Br and C atoms are centered above a surface carbon atom with the Br atom closest to the surface ($\Theta = 180°$);

(iv) the molecule is positioned above a six-membered ring and tilted 45° such that two F atoms are closest to the surface ($\Theta = 45°$).

As shown in Figure 2 the agreement between the classical trajectory (initialized without vibrational energy) and the quantum wave packet (initially in the ground state) is indeed very good. Case iv is an example where the molecule impacts at an angled geometry, which is the generic case when we later sample over initial orientations. Obviously, such an angle will not only excite modes of C_{3v} symmetry. The TDGH-DVR scheme, which includes also the other six modes (classically treated), is no longer on equal footing with the 3D wave packet treatment, and the corresponding energy transfer is therefore not included in Figure 2. The TDGH-DVR results presented are obtained using a very small grid: $15 \times 9 \times 7$ points for ν_3, ν_2, and ν_1, respectively. The results are still quite good, which is also shown in Table 1 where the energy partitioning between the modes is presented for case i. The excitation is unusually large for this collision, and it is therefore a suitable test case. The TDGH-DVR result presented is an average computed between 0.65 and 1.00 ps.

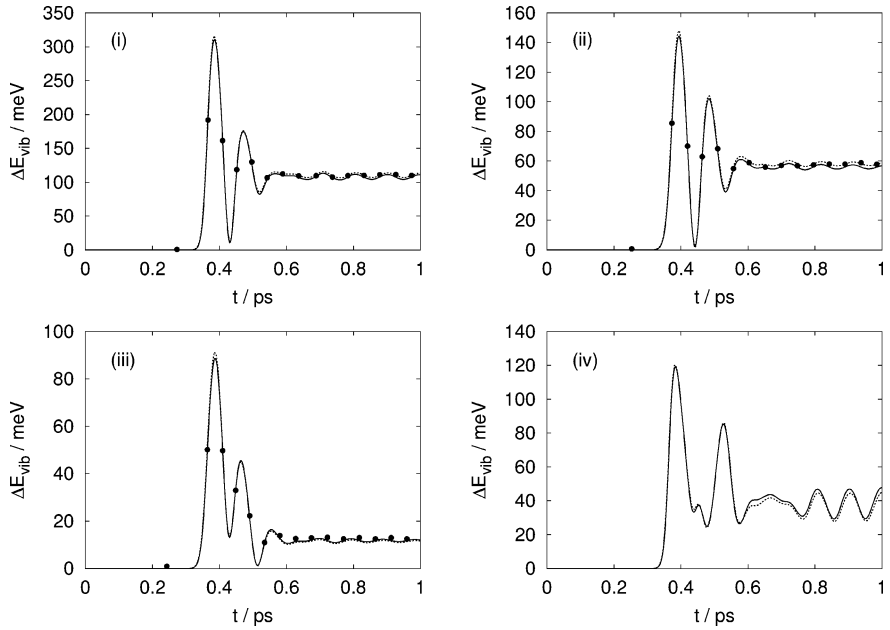

Figure 2. Vibrational excitation energy as a function of time for initial molecular orientations (i), (ii), (iii), and (iv). Results are shown for different dynamical treatments: 3D classical (solid line); 3D wave packet (dotted line); 3D TDGH-DVR (filled circles).

TABLE 1: Excitation Energies of the a_1 Modes for Initial Orientation (i) Obtained Using a Full-Dimensional Classical Trajectory (CM9D), Classical (CM3D) and Wave Packet (WP3D) Reduced Dimensionality Treatments, and the TDGH-DVR Method with the a_1 Modes Described Quantum Mechanically (GH3D)

	ΔE_{vib}/meV		
method	ν_3	ν_2	ν_1
CM9D	100.7	7.8	0.8
CM3D	100.8	7.9	0.8
WP3D	104.9	5.4	0.2
GH3D	103.0	5.5	0.9

TABLE 2: Excitation of the ν_3 Mode for Initial Orientation (i)[a]

n	GH	WP
0	8.11×10^{-2}	8.14×10^{-2}
1	2.03×10^{-1}	2.01×10^{-1}
2	2.48×10^{-1}	2.45×10^{-1}
3	2.00×10^{-1}	1.99×10^{-1}
4	1.18×10^{-1}	1.21×10^{-1}
5	5.40×10^{-2}	5.90×10^{-2}
6	2.01×10^{-2}	2.43×10^{-2}
7	6.21×10^{-3}	8.61×10^{-3}

[a] Transition probabilities from the ground state (0, 0, 0) to (n, 0, 0) obtained using the TDGH-DVR (GH) and wave packet (WP) methods are shown.

The quantum mechanical transition probabilities for excitation of the dominating ν_3 mode are shown in Table 2. The agreement between the wave packet and the TDGH-DVR results is quite good. Investigation of cases ii and iii shows that this is true for these collisions also, provided that the probabilities are larger than about 10^{-3}.

The almost total lack of effects due to a quantum treatment of the vibrations is in agreement with our previous 2D results.[6] Using the TDGH-DVR scheme as reference method we have investigated whether quantum effects become more pronounced for molecules of lower mass. This was done by artificially scaling the C, F, and Br masses with a factor f, first a factor of 2 ($f = 0.5$) and in a second step a factor of 4 ($f = 0.25$). The collision velocity was now increased to 2798 m/s in all three cases corresponding to translational energies equal to 6.0, 3.0, and 1.5 eV, respectively. Lowering the masses increases the normal mode frequencies by a factor of $\sqrt{2}$ and 2, respectively. For this study we used a grid consisting of $21 \times 21 \times 21$ points in the TDGH-DVR calculations in order to improve the accuracy of the projection. The classical results are obtained using the full-dimensional molecular dynamics program, i.e., the classical and TDGH-DVR trajectories are identical in all respects. The initial orientation of the molecule was given by case i, and the three doubly degenerate e modes were therefore not excited. The result is shown in Table 3. For this high collision velocity the instantaneous excitation at impact is very high—over 1.3 eV for $f = 1$. Neither the classical nor the TDGH-DVR estimates of the mode-resolved energy transfer are expected to be very accurate for these collisions, but it should be possible to see trends. For $f = 1$ quantum mechanics seems to lower the excitation of the ν_1 mode. Decreasing the mass ($f = 0.5$) changes $\tilde{\nu}_2$ and $\tilde{\nu}_1$ to 1078 and 1534 cm^{-1}, respectively, making them less accessible to excitation. The low-frequency mode at 498 cm^{-1} now absorbs more energy yielding a total excitation similar to the case of $f = 1$. A tendency to lower excitation of the high-frequency modes in the quantum case is observed. A further decrease of the mass ($f = 0.25$) changes the frequencies to 704, 1524, and 2170 cm^{-1}, which has a strong effect on the total energy transfer. The excitation of the ν_3 mode decreases by a factor of 2.7 both in the classical and the quantum cases, and the excitation of the high-frequency modes is negligible.

TABLE 3: Excitation Energies (in meV) of the a_1 Modes for Initial Orientation (i)[a] Obtained Using Classical Trajectories (CM) and the TDGH-DVR Method with the a_1 Modes Described Quantum Mechanically (GH)

	CM			GH		
f	ν_3	ν_2	ν_1	ν_3	ν_2	ν_1
1.00	206	47	43	196	44	32
0.50	236	26	5	248	22	4
0.25	87	2	0	91	3	1

[a] The collision velocity was 2798 ms^{-1}, and the C, F, and Br masses were scaled by a factor f.

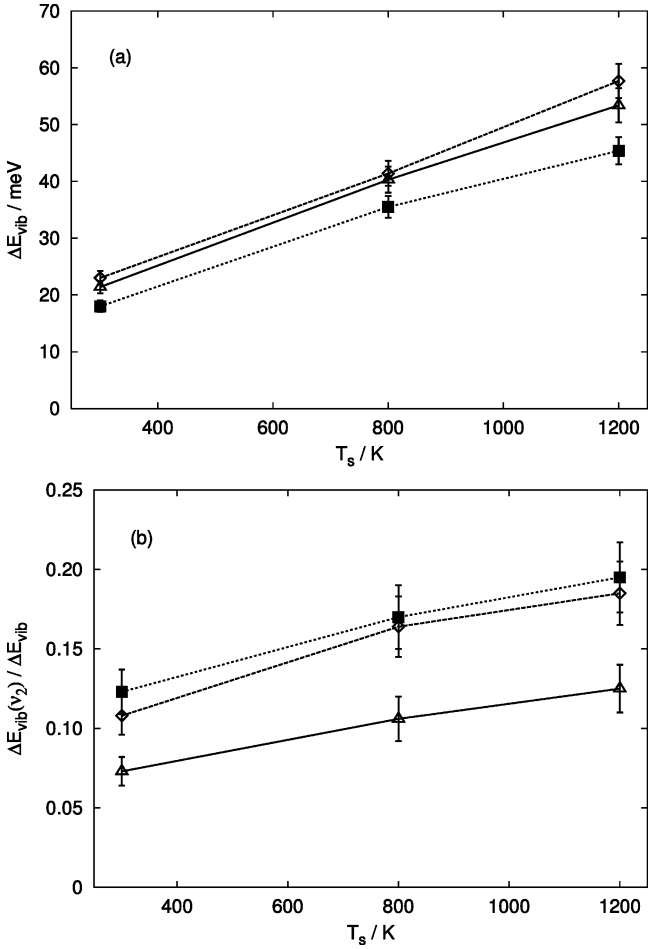

Figure 3. Surface temperature dependence of the energy transfer. In (a) the total vibrational excitation of the ν_2 and ν_3 modes is shown for classical calculations in 2D (triangles); 3D (diamonds); and 9D (squares). In (b) the ratio between the excitation of ν_2 and the total excitation of the ν_2 and ν_3 modes are shown. The error bars correspond to 95% confidence intervals.

3.2. Surface Temperature Dependence. In our previous paper[6] we also investigated the energy transfer to CF_3Br scattering from graphite at different temperatures. Comparison between classical results obtained using full-dimensional and reduced dimensional calculations showed differences regarding the distribution of energy between the ν_3 and ν_2 modes. This is an effect of the umbrella Hamiltonian used in our previous work. The C−F stretches (ν_1) are indeed stiff vibrations which are excited to a very small extent, but by including the C−F motion in the dynamical description, the ν_2 mode becomes more accessible to excitation. The classical 2D results are compared with the present 3D results in Figure 3 together with the corresponding data from full-dimensional (9D) calculations. The results are based on 2000 directly scattered trajectories per temperature. The initial translational energy was 2.0 eV (normal incidence), the initial rotational energy sampled from a 200 K distribution (random initial orientation), and the trajectories were initialized without any vibrational energy. Figure 3a shows that the total energy transferred to the ν_2 and ν_3 modes is almost identical for the 2D and 3D calculations, whereas the corresponding 9D result is somewhat lower. This is expected due to the presence of seven other vibrations which act as shock absorbers. The fraction of vibrational excitation energy going into the ν_2 mode is for the 3D model in almost perfect agreement with the 9D result, as shown in Figure 3b.

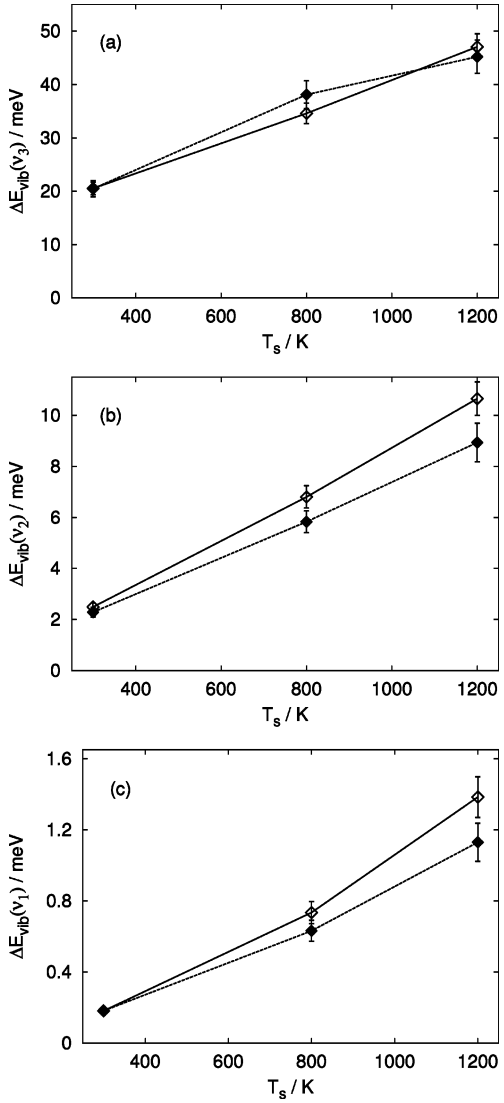

Figure 4. Average energy transfer as a function of surface temperature obtained using the 3D reduced dimensionality model. Classical results as open diamonds and wave packet results as filled diamonds for the ν_3 mode (a); the ν_2 mode (b); and the ν_1 mode (c). The error bars correspond to 95% confidence intervals.

The above comparison shows that the 3D reduced dimensionality model accurately describes the classical dynamics of the a_1 modes in CF_3Br. The mode-resolved energy transfer is compared to results from 3D wave packet calculations in Figure 4. The quantum results are averaged over 1000 wave packets for each temperature. As expected from the results in section 3.1 the agreement between the quantum and classical results is good. Excitation of the ν_3 mode dominates the energy transfer process, and the quantum and classical results are almost identical for this low-frequency mode, Figure 4a. The linear dependence on the surface temperature is in agreement with full-dimensional trajectory results and experimental data.[4] The energy transfer to the high-frequency modes is much smaller: ν_2 is a factor of 4−8 below ν_3, and the ν_1 mode is a factor of 30−100 times smaller.

The present reduced dimensionality results can, of course, not be directly compared to experimental data. The agreement between classical and quantum mechanical energy transfer (Figures 2 and 4 and Table 1) for frequencies in a range from 303 cm^{-1} to 1085 cm^{-1} strongly supports the use of classical mechanics for the 3D reduced dimensionality model. Furthermore, as implied by Figure 3 and Table 4 this is likely to carry

TABLE 4: Mode-Resolved Vibrational Excitation of CF_3Br Colliding with an 800 K Graphite Surface at 2.0 eV[a]

		ΔE_{vib}/meV		
mode	$\tilde{\nu}$/cm^{-1}	CM9D	CM3D	WP3D
$\nu_6(e)$	302.7	55.3		
$\nu_3(a_1)$	352.1	29.5	34.6	38.1
$\nu_5(e)$	547.4	21.9		
$\nu_2(a_1)$	762.0	6.1	6.8	5.8
$\nu_1(a_1)$	1084.8	0.9	0.7	0.6
$\nu_4(e)$	1208.8	1.4		

[a] Comparison of full-dimensional classical calculations (CM9D) with classical (CM3D) and wave packet (WP3D) results including the a_1 modes.

over to the full 9D treatment which is in fair agreement with experimental results.[4,6] Out of the nine vibrations the three with frequencies below 353 cm^{-1} account for 74% of the excitation (evenly distributed with ca. 28 meV per vibration). According to the analysis of the ν_3 mode, Figure 4, these should behave very classically. About 19% of the energy ends up in the ν_5 vibrations which we also expect to be well described classically. Judging from Figure 4, ν_2 and ν_1 may show a small quantum effect, but these modes only account 6% of the total vibrational excitation. Only 1% of the energy ends up in the highest frequency vibrations (ν_4).

4. Conclusions

The vibrational excitation of CF_3Br in collisions with graphite has been studied using mixed quantum−classical methods. A previously investigated reduced dimensionality treatment of the CF_3Br intramolecular dynamics has been extended to include all three totally symmetric vibrations. Addition of the high-frequency ν_1 mode (C−F stretch) has a small effect on the total excitation, which is dominated by energy transfer to the ν_3 mode (C−Br stretch). Removing the constraint of fixed C−F bond lengths significantly affects the excitation of the ν_2 (umbrella) mode.

Mixed quantum−classical calculations employing the reduced dimensionality model has been carried out using a 3D wave packet approach within a mean-field approximation. Comparisons of the quantum energy transfer with the corresponding results from classical trajectories initialized without vibrational energy show a remarkable agreement, in particular for the low-frequency mode, but the agreement is quite good even for the two higher frequencies. The present results reinforce our earlier conclusion that vibrational excitation of polyatomic molecules in their vibrational ground state can be well described using classical mechanics.

In this work we have also considered an alternative approach—the TDGH-DVR, or quantum dressed classical mechanics method. Using rather modest basis sets (few DVR points) we obtained values for the energy transfer in good agreement with the wave packet results. We also used the TDGH-DVR method to investigate how lower molecular mass affected the agreement between quantum and classical mechanics. No significant quantum effects were observed even for vibrational frequencies in the range of 704−2170 cm^{-1} indicating that classical MD may suffice also for lighter molecules.

When the TDGH-DVR method is used, all degrees of freedom are included, treated either classically or quantum mechanically. The artificial dynamical constraints connected with reduced dimensionality methods are not needed, and the quality of the quantum mechanical treatment of a particular degree of freedom can be adjusted for optimum efficiency. For bound systems the number of grid points required to obtain reasonably accurate results is surprisingly small due to the fact that the points follow the classical trajectory. These are very attractive features which deserve to be investigated in more detail.

Acknowledgment. Part of this work was presented at the symposium in memory of Professor Gert Due Billing in Copenhagen, August 11−13, 2003. This research is supported by the Swedish Research Council.

References and Notes

(1) Någård, M. B.; Andersson, P. U.; Marković, N.; Pettersson, J. B. C. *J. Chem. Phys.* **1998**, *109*, 10339.
(2) Tomsic, A.; Marković, N.; Pettersson, J. B. C. *Phys. Chem. Chem. Phys.* **2001**, *3*, 3667.
(3) Andersson, M. B.; Pettersson, J. B. C.; Marković, N. *Surf. Sci.* **1997**, *384*, L880.
(4) Någård, M. B.; Marković, N.; Pettersson, J. B. C. *J. Chem. Phys.* **1998**, *109*, 10350.
(5) Marković, N.; Andersson, P. U.; Någård, M. B.; Pettersson, J. B. C. *Chem. Phys.* **1999**, *247*, 413; *Chem. Phys.* **2000**, *252*, 409 erratum.
(6) Bäck, A.; Marković, N. *Chem. Phys.* **2002**, *285*, 233; *Chem. Phys.* **2003**, *286*, 431 corrigendum.
(7) Adhikari, S.; Billing G. D. *J. Chem. Phys* **2000**, *113*, 1409.
(8) Billing, G. D.; Adhikari, S. *Chem. Phys. Lett.* **2000**, *321*, 197.
(9) Billing, G. D. *Chem. Phys.* **2001**, *264*, 71.
(10) Billing, G. D. *J. Chem. Phys.* **2001**, *114*, 6641.
(11) Billing, G. D. *Int. J. Quantum Chem.* **2001**, *84*, 467.
(12) Coletti, C.; Billing, G. D. *Chem. Phys. Lett.* **2001**, *342*, 65.
(13) Billing, G. D. *Chem. Phys. Lett.* **2001**, *343*, 130.
(14) Billing, G. D. *Phys. Chem. Chem. Phys.* **2002**, *4*, 2865.
(15) Coletti, C.; Billing, G. D. *Chem. Phys. Lett.* **2003**, *368*, 289.
(16) Billing, G. D. *The Quantum Classical Theory*; Oxford University Press: New York, 2003.
(17) Brenner, D. W. *Phys. Rev. B* **1990**, *42*, 9458; *Phys. Rev. B* **1992**, *46*, 1948 erratum.
(18) Palma, J.; Clary, D. C. *J. Chem. Phys.* **2000**, *112*, 1859.
(19) Feit, M. D.; Fleck, J. A.; Steiger, A. *J. Comput. Phys.* **1982**, *47*, 412.
(20) Kosloff, D.; Kosloff, R. *J. Comput. Phys.* **1983**, *52*, 35.
(21) Billing, G. D. *J. Chem. Phys.* **1997**, *107*, 4286.
(22) Billing, G. D. *Chem. Phys. Lett.* **2001**, *339*, 237.
(23) Park, T. J.; Light, J. C. *J. Chem. Phys.* **1986**, *85*, 5870.